

Hybrid Textures of the Right-Handed Majorana Neutrino Mass Matrix

S. Dev^{*a,b}, Radha Raman Gautam^{†a} and Lal Singh^{‡a}

^a*Department of Physics, Himachal Pradesh University, Shimla 171005, INDIA.*

^b*Department of Physics, School of Sciences, HNBG Central University, Srinagar, Uttarakhand 246174, INDIA.*

Abstract

We perform a systematic study of neutrino mass matrices having a vanishing cofactor and an equality between two cofactors of the mass matrix. Such texture structures of the effective neutrino mass matrix arise from type-I seesaw mechanism when the Dirac neutrino mass matrix is diagonal with equal elements and the right-handed Majorana neutrino mass matrix has hybrid textures with one equality of matrix elements and one zero matrix element. For three right-handed neutrinos there are sixty possible hybrid textures out of which only six are excluded by the present experimental data. We show that such textures can be derived using discrete symmetries. The predictions of experimentally allowed textures are examined for unknown parameters such as the effective Majorana mass of the electron neutrino and the Dirac-type CP-violating phase.

1 Introduction

During the past decade various neutrino oscillation experiments have determined the neutrino mass squared differences and the lepton mixing angles with a good precision [1]. Especially the reactor mixing angle (θ_{13}) has been measured rather precisely in recent experiments[2, 3, 4, 5, 6]. The best fit value for θ_{13} is around 9° which has a large deviation from zero and provides an opportunity for the measurement of Dirac-type CP-violating phase (δ) in the lepton mixing

*dev5703@yahoo.com

†gautamrrg@gmail.com

‡lalsingh96@yahoo.com

matrix. Several ideas have been mooted to accommodate the observed pattern of neutrino mass squared differences and mixing angles which include tribimaximal (TBM) mixing [7] where one obtains fixed values of mixing angles and the neutrino masses are independent of the mixing angles. Such textures have been called mass independent textures [8]. On the other hand, zero textures [9, 10] and vanishing minors [11, 12] which relate neutrino masses with mixing angles are called mass-dependent textures. Hybrid textures which imply one equality between matrix elements and one zero element in the neutrino mass matrix also fall in the category of mass dependent textures and have been studied earlier in a basis where the charged lepton mass matrix is diagonal [13, 14, 15] and in a basis where both the charged lepton and the neutrino mass matrix have hybrid textures [16]. In the present work, we examine the phenomenological implications of hybrid textures of the inverse neutrino mass matrix in a basis where the charged lepton mass matrix is diagonal.

To understand the smallness of neutrino masses as compared to charged fermion masses, the seesaw mechanism [17] is regarded as the prime candidate. In the framework of type-I seesaw mechanism, the effective Majorana neutrino mass matrix is given by

$$M_\nu \approx -M_D M_R^{-1} M_D^T \quad (1)$$

where M_D is the Dirac neutrino mass matrix and M_R is the right-handed Majorana mass matrix. In the framework of type-I seesaw mechanism, M_ν is a quantity derived from M_D and M_R . Thus, in the context of type-I seesaw mechanism, the zeros and equalities of M_D and M_R are more fundamental. In a basis where M_D is diagonal, the zero textures of M_R show as vanishing cofactors in M_ν [11] and the equalities in M_R propagate as equal cofactors in M_ν provided that there are equal non-zero elements in diagonal M_D [18]. We consider another possibility where M_R has hybrid textures in a basis where M_D is diagonal with one equality between diagonal elements. Such M_D and M_R give rise to the neutrino mass matrix having one equality between the cofactors and one vanishing cofactor. The equality between the cofactors and the vanishing cofactor in M_ν are corresponding to the equal and zero elements of M_R . Such textures can also be seen as hybrid textures of the inverse M_ν . Thus, effectively we are studying the hybrid textures of M_ν^{-1} . For three right-handed neutrinos, there are sixty possible hybrid textures of M_R which are listed in Table 1. To illustrate how such textures can be realised we present a flavor model for class *IA* using discrete flavor symmetries.

2 The Neutrino Mass Matrix

Assuming neutrinos to be Majorana particles, we reconstruct the neutrino mass matrix in the flavor basis (where the charged lepton mass matrix “ M_l ” is diagonal). In this basis, the complex symmetric neutrino mass matrix is diagonalized by a unitary matrix V' as

$$M_\nu = V' M_\nu^{diag} V'^T \quad (2)$$

where $M_\nu^{diag} = \text{diag}(m_1, m_2, m_3)$.

The unitary matrix V' can be parametrized as

$$V' = P_l V \quad \text{with} \quad V = U P_\nu \quad (3)$$

where [19]

$$U = \begin{pmatrix} c_{12}c_{13} & s_{12}c_{13} & s_{13}e^{-i\delta} \\ -s_{12}c_{23} - c_{12}s_{23}s_{13}e^{i\delta} & c_{12}c_{23} - s_{12}s_{23}s_{13}e^{i\delta} & s_{23}c_{13} \\ s_{12}s_{23} - c_{12}c_{23}s_{13}e^{i\delta} & -c_{12}s_{23} - s_{12}c_{23}s_{13}e^{i\delta} & c_{23}c_{13} \end{pmatrix} \quad (4)$$

with $s_{ij} = \sin \theta_{ij}$ and $c_{ij} = \cos \theta_{ij}$ and

$$P_\nu = \begin{pmatrix} 1 & 0 & 0 \\ 0 & e^{i\alpha} & 0 \\ 0 & 0 & e^{i(\beta+\delta)} \end{pmatrix}, \quad P_l = \begin{pmatrix} e^{i\varphi_e} & 0 & 0 \\ 0 & e^{i\varphi_\mu} & 0 \\ 0 & 0 & e^{i\varphi_\tau} \end{pmatrix}.$$

P_ν is the diagonal phase matrix with two Majorana-type CP-violating phases α , β and one Dirac-type CP-violating phase δ . The phase matrix P_l is not observable and depends on the phase convention. The matrix V is called the neutrino mixing matrix or the Pontecorvo-Maki-Nakagawa-Sakata (PMNS) matrix [20]. Using Eq. (2) and Eq. (3), the neutrino mass matrix can be written as

$$M_\nu = P_l U P_\nu M_\nu^{diag} P_\nu^T U^T P_l^T. \quad (5)$$

The CP-violation in neutrino oscillation experiments can be described through a rephasing invariant quantity, J_{CP} [21] with $J_{CP} = \text{Im}(U_{e1}U_{\mu 2}U_{e2}^*U_{\mu 1}^*)$. In the above parametrization, J_{CP} is given by

$$J_{CP} = s_{12}s_{23}s_{13}c_{12}c_{23}c_{13}^2 \sin \delta. \quad (6)$$

2.1 Neutrino Mass Matrices with an Equality Between the Cofactors and a Vanishing Cofactor

In the effective neutrino mass matrix, the simultaneous existence of an equality between two cofactors and one vanishing cofactor implies

$$\begin{aligned} & (-1^{(\gamma\xi)})(e^{i(\varphi_a+\varphi_b+\varphi_c+\varphi_d)} M_{\nu(ab)} M_{\nu(cd)} - e^{i(\varphi_f+\varphi_g+\varphi_m+\varphi_n)} M_{\nu(fg)} M_{\nu(mn)}) - \\ & (-1^{(\zeta\eta)})(e^{i(\varphi_p+\varphi_q+\varphi_r+\varphi_s)} M_{\nu(pq)} M_{\nu(rs)} - e^{i(\varphi_t+\varphi_u+\varphi_v+\varphi_w)} M_{\nu(tu)} M_{\nu(vw)}) = 0 \end{aligned} \quad (7)$$

$$e^{i(\varphi_{a'}+\varphi_{b'}+\varphi_{c'}+\varphi_{d'})} M_{\nu(a'b')} M_{\nu(c'd')} - e^{i(\varphi_{f'}+\varphi_{g'}+\varphi_{m'}+\varphi_{n'})} M_{\nu(f'g')} M_{\nu(m'n')} = 0. \quad (8)$$

The condition for equality between two cofactors in the neutrino mass matrix [Eq. (7)] can be written as

$$\begin{aligned} & (-1^{(\gamma\xi)})(Q_1 M_{\nu(ab)} M_{\nu(cd)} - Q_2 M_{\nu(fg)} M_{\nu(mn)}) - \\ & (-1^{(\zeta\eta)})(Q_3 M_{\nu(pq)} M_{\nu(rs)} - Q_4 M_{\nu(tu)} M_{\nu(vw)}) = 0. \end{aligned} \quad (9)$$

It is inherent in the properties of cofactors that when we substitute φ_j , ($j = e, \mu, \tau$), then $Q_1 = Q_2$ and $Q_3 = Q_4$. Thus, we have

$$\begin{aligned} & (-1^{(\gamma\xi)})Q_1(M_{\nu(ab)}M_{\nu(cd)} - M_{\nu(fg)}M_{\nu(mn)}) - \\ & (-1^{(\zeta\eta)})Q_3(M_{\nu(pq)}M_{\nu(rs)} - M_{\nu(tu)}M_{\nu(vw)}) = 0. \end{aligned} \quad (10)$$

or

$$\begin{aligned} & (-1^{(\gamma\xi)})Q(M_{\nu(ab)}M_{\nu(cd)} - M_{\nu(fg)}M_{\nu(mn)}) - \\ & (-1^{(\zeta\eta)})(M_{\nu(pq)}M_{\nu(rs)} - M_{\nu(tu)}M_{\nu(vw)}) = 0. \end{aligned} \quad (11)$$

where $Q = \frac{Q_1}{Q_3}$.

The two conditions Eq.(8) and Eq.(11) take the following form when expressed in terms of the mixing matrix elements and mass eigenvalues:

$$\begin{aligned} & \sum_{k,l=1}^3 \{(-1^{(\gamma\xi)})Q(V_{ak}V_{bk}V_{cl}V_{dl} - V_{fk}V_{gk}V_{ml}V_{nl}) - \\ & (-1^{(\zeta\eta)})(V_{pk}V_{qk}V_{rl}V_{sl} - V_{tk}V_{uk}V_{vl}V_{wl})\}m_k m_l = 0, \end{aligned} \quad (12)$$

$$\sum_{k,l=1}^3 (V_{a'k}V_{b'k}V_{c'l}V_{d'l} - V_{f'k}V_{g'k}V_{m'l}V_{n'l})m_k m_l = 0. \quad (13)$$

The above equations can be rewritten as

$$m_1 m_2 A_3 e^{2i\alpha} + m_2 m_3 A_1 e^{2i(\alpha+\beta+\delta)} + m_3 m_1 A_2 e^{2i(\beta+\delta)} = 0, \quad (14)$$

$$m_1 m_2 B_3 e^{2i\alpha} + m_2 m_3 B_1 e^{2i(\alpha+\beta+\delta)} + m_3 m_1 B_2 e^{2i(\beta+\delta)} = 0 \quad (15)$$

where

$$\begin{aligned} A_h &= (-1^{(\gamma\xi)})Q(U_{ak}U_{bk}U_{cl}U_{dl} - U_{fk}U_{gk}U_{ml}U_{nl}) - \\ & (-1^{(\zeta\eta)})(U_{pk}U_{qk}U_{rl}U_{sl} - U_{tk}U_{uk}U_{vl}U_{wl}) + (k \leftrightarrow l), \end{aligned} \quad (16)$$

$$B_h = (U_{a'k}U_{b'k}U_{c'l}U_{d'l} - U_{f'k}U_{g'k}U_{m'l}U_{n'l}) + (k \leftrightarrow l) \quad (17)$$

with (h, k, l) as the cyclic permutation of $(1, 2, 3)$. The two complex Eqs.(14) and (15) contain nine physical parameters which are the three neutrino masses (m_1, m_2, m_3) , the three mixing angles $(\theta_{12}, \theta_{23}, \theta_{13})$ and three CP-violating phases (α, β, δ) . In addition, there are three unobservable phases $(\varphi_e, \varphi_\mu, \varphi_\tau)$ which enter in the mass ratios as a phase difference. The masses m_2 and m_3 can be calculated from the mass-squared differences Δm_{21}^2 ($\Delta m_{21}^2 \equiv m_2^2 - m_1^2$) and $|\Delta m_{32}^2|$ using the following relations

$$m_2 = \sqrt{m_1^2 + \Delta m_{21}^2}, \quad m_3 = \sqrt{m_2^2 + |\Delta m_{32}^2|} \quad (18)$$

with $m_2 > m_3$ for an Inverted Spectrum (IS) and $m_2 < m_3$ for the Normal Spectrum (NS). By using the experimental inputs of the two mass-squared differences and the three mixing

angles, we can constrain the other parameters. Simultaneously solving Eqs.(14) and (15) for the two mass ratios, we obtain

$$\frac{m_1}{m_2} e^{-2i\alpha} = \frac{A_3 B_2 - A_2 B_3}{A_1 B_3 - A_3 B_1}, \quad (19)$$

$$\frac{m_1}{m_3} e^{-2i\beta} = \frac{A_2 B_3 - A_3 B_2}{A_1 B_2 - A_2 B_1} e^{2i\delta}. \quad (20)$$

We denote the magnitudes of the above two mass ratios by

$$\rho = \left| \frac{m_1}{m_3} e^{-2i\beta} \right|, \quad (21)$$

$$\sigma = \left| \frac{m_1}{m_2} e^{-2i\alpha} \right|. \quad (22)$$

The Majorana-type CP-violating phases α and β are given by

$$\alpha = -\frac{1}{2} \arg \left(\frac{A_3 B_2 - A_2 B_3}{A_1 B_3 - A_3 B_1} \right), \quad (23)$$

$$\beta = -\frac{1}{2} \arg \left(\frac{A_2 B_3 - A_3 B_2}{A_1 B_2 - A_2 B_1} e^{2i\delta} \right). \quad (24)$$

Since, Δm_{21}^2 and $|\Delta m_{32}^2|$ are experimentally known, the two mass ratios (ρ, σ) in Eqs.(21) and (22) can be used to calculate m_1 . This can be done by inverting Eq.(18) to obtain the two values of m_1 , viz.

$$m_1 = \sigma \sqrt{\frac{\Delta m_{21}^2}{1 - \sigma^2}}, \quad m_1 = \rho \sqrt{\frac{\Delta m_{21}^2 + |\Delta m_{32}^2|}{1 - \rho^2}}. \quad (25)$$

There exists a permutation symmetry between different patterns of two-zero textures [10], in the case of two vanishing minors [12] and in the case of two equalities in M_ν [18]. Similarly, there exists a permutation symmetry between different hybrid textures of M_ν^{-1} . The permutation matrix is given by

$$P_{23} = \begin{pmatrix} 1 & 0 & 0 \\ 0 & 0 & 1 \\ 0 & 1 & 0 \end{pmatrix}. \quad (26)$$

For example, the neutrino mass matrix for class *IC* can be obtained from class *IB* by the transformation

$$M_\nu^{IC} = P_{23} M_\nu^{IB} P_{23}^T. \quad (27)$$

This leads to the following relations between the parameters of the classes related by the 2-3 permutation symmetry:

$$\theta_{12}^{IC} = \theta_{12}^{IB}, \quad \theta_{13}^{IC} = \theta_{13}^{IB}, \quad \theta_{23}^{IC} = \frac{\pi}{2} - \theta_{23}^{IB}, \quad \delta^{IC} = \delta^{IB} - \pi. \quad (28)$$

The textures related by the 2-3 permutation symmetry are:

$$\begin{aligned}
& IB \leftrightarrow IC, ID \leftrightarrow IIF, IE \leftrightarrow IIE, IF \leftrightarrow IID, IIA \leftrightarrow VIIA, IIB \leftrightarrow IVC, IIC \leftrightarrow IVB, \\
& IIIA \leftrightarrow VIA, IIIB \leftrightarrow IIIC, IIID \leftrightarrow IVF, IIIE \leftrightarrow IVE, IIIF \leftrightarrow IVD, IVA \leftrightarrow VA, \\
& VB \leftrightarrow VIIC, VC \leftrightarrow VIIB, VD \leftrightarrow VF, VIB \leftrightarrow VIC, VID \leftrightarrow IXF, VIE \leftrightarrow IXE, \\
& VIF \leftrightarrow IXD, VIID \leftrightarrow VIIF, VIIE \leftrightarrow VIIE, VIIF \leftrightarrow VIID, VIIIA \leftrightarrow XA, \\
& VIIIB \leftrightarrow XC, VIIIC \leftrightarrow XB, IXB \leftrightarrow IXC, XD \leftrightarrow XF.
\end{aligned} \tag{29}$$

The remaining textures namely:

$$IA, VE, IXA, XE \tag{30}$$

transform unto themselves.

3 Numerical Analysis and Results

The latest global fit results on neutrino oscillation parameters at 1, 2 and 3σ [22] are summarised in Table 2. The effective Majorana mass of the electron neutrino (M_{ee}) which determines the rate of neutrinoless double beta (NDB) decay is given by

$$M_{ee} = |m_1 c_{12}^2 c_{13}^2 + m_2 s_{12}^2 c_{13}^2 e^{2i\alpha} + m_3 s_{13}^2 e^{2i\beta}|. \tag{31}$$

Observation of NDB decay will imply that neutrinos are Majorana fermions. NDB decay also provides a way to probe the neutrino mass scale. There are a large number of projects such as CUORICINO[23], CUORE [24], GERDA [25], MAJORANA [26], SuperNEMO [27], EXO [28], GENIUS [29] which aim to achieve a sensitivity upto 0.01 eV for M_{ee} . We take the upper limit of M_{ee} to be 0.5 eV [30]. In addition, cosmological observations put an upper bound on the sum of light neutrino masses

$$\Sigma = \sum_{i=1}^3 m_i. \tag{32}$$

Recent data from Planck satellite [31] combined with other cosmological data limit $\Sigma < 0.23$ at 95% Confidence level. However, these bounds are strongly dependent on model details and the data set used. Thus, in our numerical analysis we take the upper limit on Σ to be 1 eV. In our numerical programs, the constraints implied by an equality between the two cofactors of M_ν and one vanishing cofactor in M_ν are used by equating the two values of m_1 obtained in Eq. (25). These two values of m_1 should be equal to within the errors of the oscillation parameters. We vary the known oscillation parameters randomly within their 3σ experimental ranges given in [22]. The unknown Dirac-type CP-violating phase δ is varied randomly within its full possible range. For the numerical analysis, we generate 10^7 random points (10^8 when the number of allowed points is small) for the allowed 3σ ranges of oscillation parameters.

Main results of the numerical analysis are:

Parameter	Mean $\begin{matrix} (+1\sigma, +2\sigma, +3\sigma) \\ (-1\sigma, -2\sigma, -3\sigma) \end{matrix}$
$\Delta m_{21}^2 [10^{-5} eV^2]$	$7.62 \begin{matrix} (+0.19, +0.39, +0.58) \\ (-0.19, -0.35, -0.5) \end{matrix}$
$\Delta m_{31}^2 [10^{-3} eV^2]$	$2.55 \begin{matrix} (+0.06, +0.13, +0.19) \\ (-0.09, -0.19, -0.24) \end{matrix},$ $(-2.43 \begin{matrix} (+0.09, +0.19, +0.24) \\ (-0.07, -0.15, -0.21) \end{matrix})$
$\sin^2 \theta_{12}$	$0.32 \begin{matrix} (+0.016, +0.03, +0.05) \\ (-0.017, -0.03, -0.05) \end{matrix}$
$\sin^2 \theta_{23}$	$0.613 \begin{matrix} (+0.022, +0.047, +0.067) \\ (-0.04, -0.233, -0.25) \end{matrix},$ $(0.60 \begin{matrix} (+0.026, +0.05, +0.07) \\ (-0.031, -0.210, -0.230) \end{matrix})$
$\sin^2 \theta_{13}$	$0.0246 \begin{matrix} (+0.0028, +0.0056, +0.0076) \\ (-0.0029, -0.0054, -0.0084) \end{matrix},$ $(0.0250 \begin{matrix} (+0.0026, +0.005, +0.008) \\ (-0.0027, -0.005, -0.008) \end{matrix})$

Table 2: Current Neutrino oscillation parameters from global fits [22]. The upper (lower) row corresponds to Normal (Inverted) Spectrum, with $\Delta m_{31}^2 > 0$ ($\Delta m_{31}^2 < 0$).

- Six textures, viz.,
IIA, IIIA, IVA, VA, VIA and *VIIA* are excluded by the present experimental data.
- Textures *IE, IIE, IIID, IIIE, IVE, IVF, VIE, VIIE, VIIF, VIIID, VIIIE* and *IXE* lead to a normal spectrum only.
- Textures *IA, IB, IC, IIC, IIIB, IIIC, IVB, VIIIA, IXA* and *XA* lead to an inverted spectrum only.
- The allowed points for the following textures are very few for *IB, IF, IID, IIF, IIIF, IVD, VE, VID, VIIIA, IXA, IXF, XD, XE, XF* for an inverted spectrum and *IXB, IXC* for both inverted and normal spectrum. We have generated 10^8 random points for these textures.
- All the viable textures except *IA, IB, IC, VIIE, VIIIA, VIIIE* and *XA* allow quasi-degenerate spectrum.
- Many of the classes predict a constrained range for M_{ee} .
- It is found that the smallest neutrino mass cannot be zero for any of the allowed textures.
- For textures:
IIB, IIC, IIIB, IIIC, IVB, IVC, VB, VC, VD, VE, VF, VIB, VIC, VIIB, VIIC, VIIIB, VIIIC, IXB, IXC, XB, XC and *VIF*, a non-vanishing reactor mixing angle is an inherent property since for $\theta_{13} = 0$ the solar mass square difference (Δm_{21}^2) vanishes *i.e.* $m_1 = m_2$, which is contrary to the experimental observations.

We have summarised the numerical results for all the classes compatible with the present experimental data in Table 3. Some of the interesting results are plotted in Figs. 1-5. Fig.

Texture	Spectrum	M_{ee} (eV)	m_0 (eV)	θ_{23}	Majorana Phases
IA	IS	0.01-0.055	0.0007	-	$\beta = 70^\circ-110^\circ$
IB (IC)	IS	0.034-0.05	0.007	-	$\alpha=25^\circ-55^\circ, 125^\circ-155^\circ$
ID (IIF)	NS	0-0.15	0.003	-	$\alpha=50^\circ-130^\circ$
	IS	0.03-0.20	0.03	$< 45^\circ(> 45^\circ)$	$\alpha=45^\circ-165^\circ, 115^\circ-135^\circ$
IE (IIE)	NS	0-0.07	0.002	-	$\alpha=40^\circ-140^\circ$
IF (IID)	NS	0-0.16	0.002	-	$\alpha=50^\circ-130^\circ$
	IS	0.02-0.16	0.06	$> 45^\circ(< 45^\circ)$	$\alpha=60^\circ-120^\circ$
IIB (IVC)	NS	0.04-0.35	0.05	-	$\alpha=0^\circ-30^\circ, 150^\circ-180^\circ$
	IS	0.04-0.35	0.008	-	$\alpha, \beta=0^\circ-30^\circ, 150^\circ-180^\circ$
IIC (IVB)	IS	0.02-0.35	0.01	-	$\alpha=0^\circ-80^\circ, 100^\circ-180^\circ$
IIIB (IIIC)	IS	0.03-0.30	0.015	-	$\alpha=0^\circ-60^\circ, 120^\circ-180^\circ$
IIID (IVF)	NS	0.002-0.25	0.015	-	-
IIIE (IVE)	NS	0-0.35	0.01	-	$\alpha=5^\circ-175^\circ$
IIIF (IVD)	NS	0-0.16	0.01	-	$\alpha=60^\circ-120^\circ$
	IS	0.04-0.18	0.02	$> 45^\circ(< 45^\circ)$	$\alpha=0^\circ-80^\circ, 100^\circ-180^\circ$
VB (VIIC)	NS	0.004-0.35	0.005	$> 45^\circ(< 45^\circ)$	$\alpha=0^\circ-20^\circ, 160^\circ-180^\circ$
	IS	0.04-0.35	0.010	$< 45^\circ(> 45^\circ)$	$\alpha=0^\circ-20^\circ, 160^\circ-180^\circ$
VC (VIIB)	NS	0.005-0.30	0.007	$> 45^\circ(< 45^\circ)$	$\alpha=0^\circ-10^\circ, 170^\circ-180^\circ$
	IS	0.01-0.30	0.01	$< 45^\circ(> 45^\circ)$	-
VD (VF)	NS	0-0.35	0.001	-	-
	IS	0.04-0.35	0.020	-	$\alpha=0^\circ-45^\circ, 135^\circ-180^\circ$
VE	NS	0-0.20	0.001	-	-
	IS	0.1-0.35	0.10	-	$\alpha=0^\circ-10^\circ, 170^\circ-180^\circ, \beta=20^\circ-160^\circ$
VIB (VIC)	NS	0.002-0.35	0.004	-	$\alpha=0^\circ-20^\circ, 160^\circ-180^\circ$
	IS	0.02-0.35	0.013	-	$\alpha=0^\circ-80^\circ, 100^\circ-180^\circ$
VID (IXF)	NS	0.005-0.12	0.006	-	$\alpha=0^\circ-80^\circ, 100^\circ-180^\circ$
	*IS	0.03-0.14	0.04	$< 45^\circ(> 45^\circ)$	$\alpha=60^\circ-120^\circ$
VIE (IXE)	NS	0.001-0.07	0.016	-	$\alpha=40^\circ-140^\circ$
VIF (IXD)	NS	0.002-0.30	0.003	-	-
	IS	0.05-0.35	0.044	$> 45^\circ(< 45^\circ)$	$\alpha=0^\circ-80^\circ, 100^\circ-180^\circ$
VIID (VIIF)	NS	0-0.30	0.0008	$> 45^\circ(< 45^\circ)$	-
	IS	0.02-0.30	0.045	$< 45^\circ(> 45^\circ)$	-
VIII (VIII E)	NS	0.008-0.03	0.02	-	$\alpha=50^\circ-130^\circ$
VIIIF (VIIID)	NS	0.008-0.028	0.007	-	$\alpha=30^\circ-150^\circ$
VIIIA (XA)	IS	0.01-0.05	0.0008	-	$\beta=70^\circ-110^\circ$
VIIIB (XC)	NS	0.003-0.25	0.005	-	$\alpha=0^\circ-20^\circ, 160^\circ-180^\circ$
	IS	0.01-0.25	0.003	-	-
VIIIC (XB)	NS	0.003-0.25	0.005	-	$\alpha=0^\circ-20^\circ, 160^\circ-180^\circ$
	IS	0.003-0.30	0.003	-	-
IXA	IS	-	-	-	-
IXB (IXC)	NS	0.003-0.30	0.0052	$36^\circ-48^\circ(42^\circ-56^\circ)$	$\alpha=0^\circ-30^\circ, 150^\circ-180^\circ$
	IS	0.01-0.35	0.0065	$36^\circ-46^\circ(44^\circ-56^\circ)$	-
XD (XF)	NS	0.001-0.045	0.0015	-	$\alpha=20^\circ-160^\circ$
	IS	0.03-0.13	0.022	$< 45^\circ(> 45^\circ)$	$\alpha=35^\circ-145^\circ$
XE	NS	0.001-0.30	0.002	-	-
	IS	-	-	-	-

Table 3: The predictions for the phenomenologically viable textures. m_o is the lowest mass scale *i.e.* lowest value of m_1 for NS and m_3 for IS.

1(a) shows the correlation plot between the two Majorana-type phases (α and β) for class IA (IS). For class IIB (NS), δ approaches 0° or 180° with the increase in M_{ee} [Fig. 1(b)]. Also, for the normal spectrum, J_{CP} cannot be equal to zero [Fig. 1(c)] implying that CP is necessarily violated. There is an interesting correlation between θ_{12} and θ_{23} for class $IIIF$ (NS) [Fig. 1(d)] for which θ_{12} must remain below 34° when θ_{23} is above maximal. For class IVD , θ_{23} and θ_{13} are correlated [Figs. 1(e)(NS), 1(f)(IS)]. In Fig. 2, we have given correlation plots for classes VB and VC which are among the most predictive textures in this analysis. The Majorana phases are restricted to a very small range for class VB (IS) [Fig. 2(a)]. The Dirac-type phase is restricted near 90° or 270° [Fig. 2(b)] and J_{CP} is always non-zero [Fig. 2(c)] implying that, for inverted spectrum, this class is necessarily CP-violating. For class VC (NS), θ_{23} is always above 45° [Fig. 2(d)] and the Dirac-type phase is fixed near 90° and 270° for $M_{ee} > 0.05$ eV [Fig. 2(e)]. For the inverted spectrum for this class, δ again approaches 90° and 270° with increasing M_{ee} [Fig. 2(f)]. Fig. 3(a) depicts the correlation plot between δ and M_{ee} for class VE (IS). For class VIB , the Dirac-type phase δ approaches 0° and 180° with increasing M_{ee} for both normal and inverted spectra [Figs. 3(b) and 3(c)]. Fig. 3(d) shows the correlation plot between θ_{23} and θ_{13} for class VID (IS) for which θ_{23} remains below maximal for the allowed ranges of other neutrino oscillation parameters. The correlation plots between δ and M_{ee} for classes VIE and VIF for normal and inverted spectra are shown in Figs. 3(e)(NS) and 3(f)(IS). For class $VIIF$ (NS), M_{ee} is restricted to a small range 0.008-0.028 [Fig. 4(a)] and the correlation plot depicting normal spectrum for this class is shown in Fig. 4(b). For class $VIIIA$ (IS), the atmospheric mixing angle θ_{23} remains near maximal as shown in Fig. 4(c). Fig. 4(d) shows the correlation plot of δ and M_{ee} for class $VIIIB$ (NS) where for larger values of M_{ee} , the Dirac phase δ is restricted to very small ranges. Again, for class $VIIIC$ (NS), δ is restricted to very small ranges for larger values of M_{ee} [Fig. 4(e)]. Fig. 4(f) shows the correlation plot between δ and α where α has a very small allowed range near 0° and 180° [Fig. 4(f)]. The 2-3 interchange symmetry between classes $VIIF$ and VID for NS is shown in Figs. 5(a) and 5(b). In addition to the textures for which non-zero θ_{13} is an inherent property, there are other textures namely IA , $VIIIA$, IXA and XA which forbid a vanishing θ_{13} . This is because for $\theta_{13} = 0$, these textures predict

$$\left| \frac{m_1}{m_2} \right| = |-\cot^2 \theta_{12}| > 1 \quad \text{for the allowed range of } \theta_{12} \quad (33)$$

which is contrary to the experimental observations.

4 Symmetry Realization

We present a representative model for obtaining hybrid texture in the right-handed neutrino mass matrix M_R . Here we need one equality and one vanishing entry in M_R in a basis where both M_D and M_l are diagonal with additional equality in M_D . The additional equality in M_D is needed so that the equal elements of M_R may propagate as equal cofactors in M_ν . General

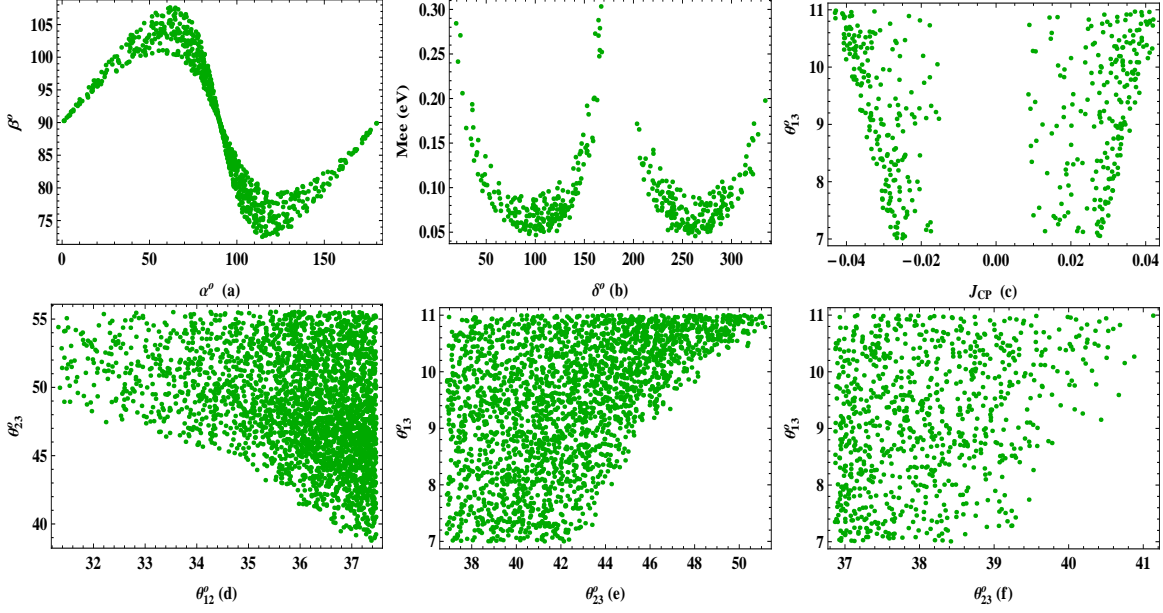


Figure 1: Correlation plots for classes $IA(IS)$ (a), $IIB(NS)$ (b, c), $IIIF(NS)$ (d), $IVD(NS)$ (e) and $IVD(IS)$ (f).

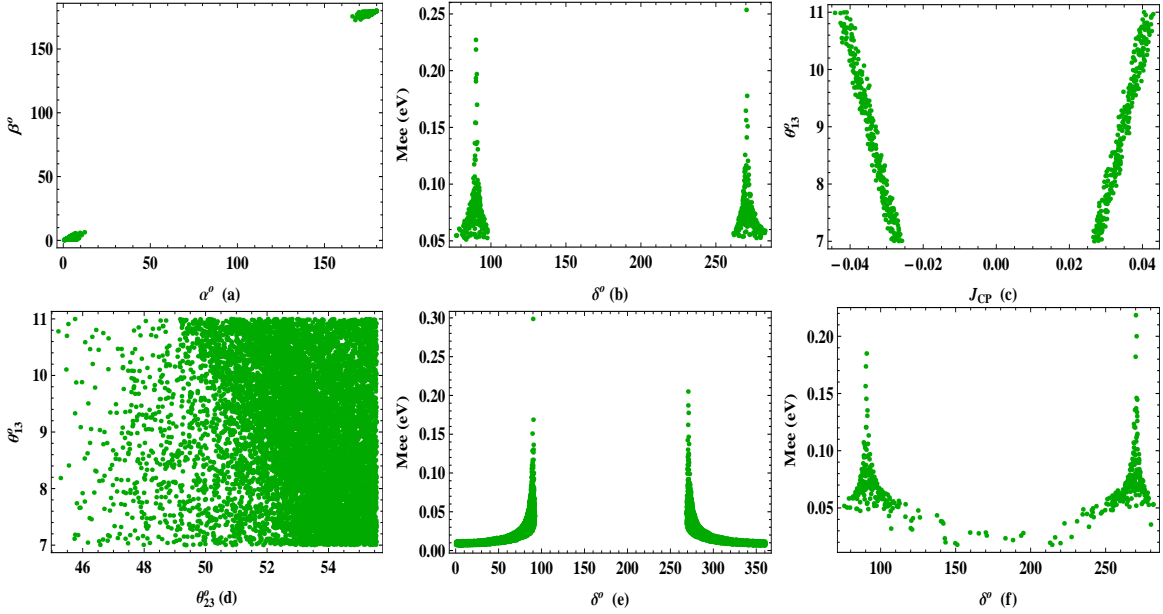


Figure 2: Correlation plots for classes $VB(IS)$ (a, b, c), $VC(NS)$ (d, e) and $VC(IS)$ (f).

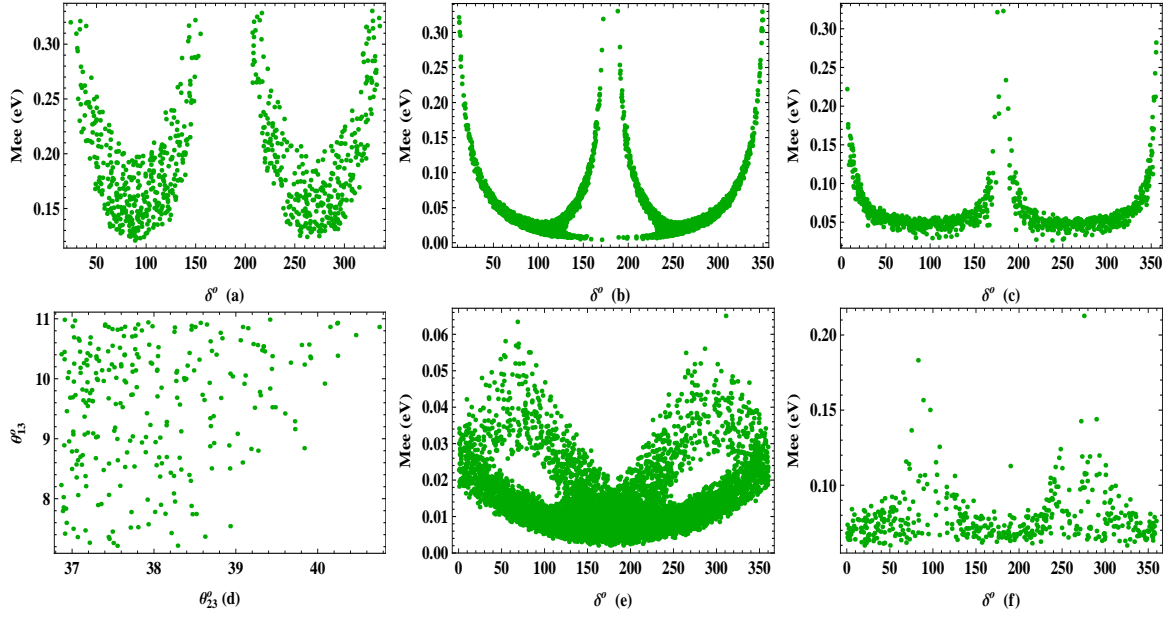


Figure 3: Correlation plots for classes $VE(IS)$ (a), $VIB(NS)$ (b), $VIB(IS)$ (c), $VID(IS)$ (d), $VIE(NS)$ (e) and $VIF(IS)$ (f).

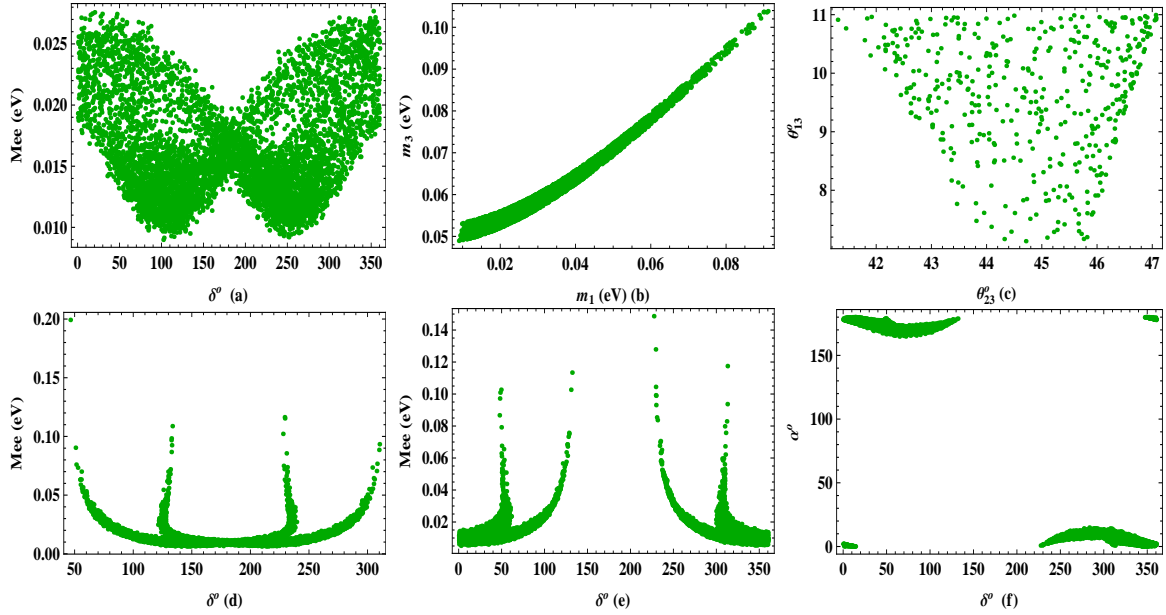


Figure 4: Correlation plots for classes $VIIF(NS)$ (a, b), $VIIIA(IS)$ (c), $VIIB(NS)$ (d) and $VIIC(NS)$ (e, f).

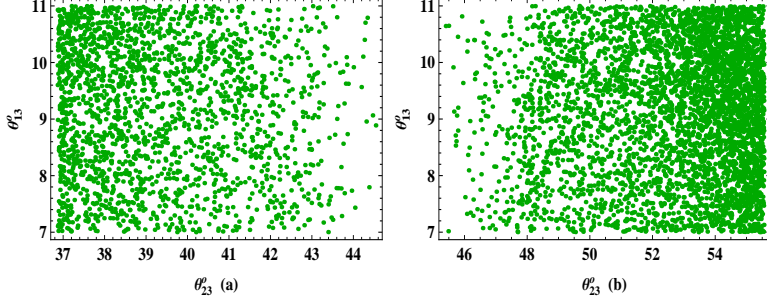


Figure 5: Correlation plots for classes $VIII F(NS)(a)$ and $VIID(NS)(b)$ depicting the 2-3 interchange symmetry.

guidelines for obtaining zero entries at any place in fermion mass matrices using Abelian discrete symmetries have been propounded in [32], in particular all the viable cases of two zero textures in the neutrino mass matrix in flavor basis have been realized in [10, 33] considering only the type-II seesaw contribution and in [34] considering both type-(I+II) seesaw contributions and using a minimal cyclic symmetry group. A few cases of hybrid textures in the effective neutrino mass matrix have been realised in [15, 35]. Here we present the symmetry realization of class IA as an illustration of how the hybrid textures of M_ν^{-1} may be realised. For this we follow the approach of Ref. [36].

In addition to the Standard Model (SM) left-handed $SU(2)$ lepton doublets $D_{\ell L}$ ($\ell = e, \mu, \tau$) and the right-handed charged-lepton $SU(2)$ singlets ℓ_R , we introduce three right-handed neutrinos $\nu_{\ell R}$. In the scalar sector we need three Higgs doublets ϕ_j ($j = 1, 2, 3$), we will also need three scalar singlets. We assume the validity of the lepton number symmetries $U(1)_{L_\ell}$ for all dimension 4 terms in the Lagrangian. This leads to diagonal charged lepton (M_l) and Dirac neutrino (M_D) mass matrices. However, the dimension 3 terms are allowed to break the L_ℓ softly.

We consider the following symmetries and transformations of various fields under these symmetries:

$$\mathbb{Z}_2 : \quad \phi_1, e_R, \nu_{\ell R} \longrightarrow -\phi_1, -e_R, -\nu_{\ell R} \quad (34)$$

$$\begin{aligned} \mathbb{Z}_4 : \quad & D_{eL} \longrightarrow -iD_{eL}, & D_{\mu L} \longrightarrow iD_{\tau L}, & D_{\tau L} \longrightarrow iD_{\mu L}, \\ & e_R \longrightarrow -ie_R, & \mu_R \longrightarrow i\tau_R, & \tau_R \longrightarrow i\mu_R, \\ & \nu_{eR} \longrightarrow -i\nu_{eR}, & \nu_{\mu R} \longrightarrow i\nu_{\tau R}, & \nu_{\tau R} \longrightarrow i\nu_{\mu R}, \\ & \phi_3 \longrightarrow -\phi_3 . \end{aligned} \quad (35)$$

These symmetries lead to the following Yukawa Lagrangian:

$$\begin{aligned} \mathcal{L}_Y = & Y_1(\overline{D}_{eL}e_R)\phi_1 + Y_2(\overline{D}_{\mu L}\mu_R + \overline{D}_{\tau L}\tau_R)\phi_2 + Y_3(\overline{D}_{\mu L}\mu_R - \overline{D}_{\tau L}\tau_R)\phi_3 + Y_4(\overline{D}_{eL}\nu_{eR})\tilde{\phi}_1 \\ & Y_5(\overline{D}_{\mu L}\nu_{\mu R} + \overline{D}_{\tau L}\nu_{\tau R})\tilde{\phi}_1 + \text{H. c.} \end{aligned} \quad (36)$$

where $\tilde{\phi}_1 = i\tau_2\phi_1^*$. When the Higgs fields (ϕ_j) acquire non-zero vacuum expectation values (VEVs), we have the charged lepton mass matrix M_l and the Dirac neutrino mass matrix M_D of the following form:

$$M_l = \text{diag}(e^{i\phi_e}m_e, e^{i\phi_\mu}m_\mu, e^{i\phi_\tau}m_\tau) \quad (37)$$

$$M_D = \text{diag}(x, y, y). \quad (38)$$

where $m_e = |Y_1\langle\phi_1\rangle_o|$, $m_\mu = |Y_2\langle\phi_2\rangle_o + Y_3\langle\phi_3\rangle_o|$, $m_\tau = |Y_2\langle\phi_2\rangle_o - Y_3\langle\phi_3\rangle_o|$, $x = Y_4\langle\phi_1^*\rangle_o$ and $y = Y_5\langle\phi_1^*\rangle_o$.

The Majorana mass terms for the right-handed neutrinos, invariant under above symmetries are

$$\mathcal{L}_M = \frac{M_1}{2}\nu_{eR}^T C^{-1}(\nu_{\mu R} + \nu_{\tau R}) + \frac{M_2}{2}(\nu_{\mu R}^T C^{-1}\nu_{\mu R} - \nu_{\tau R}^T C^{-1}\nu_{\tau R}) + \text{H. c.} \quad (39)$$

These mass terms lead to a right-handed Majorana mass matrix having the following form

$$M_R = \begin{pmatrix} 0 & a & a \\ a & b & 0 \\ a & 0 & -b \end{pmatrix}. \quad (40)$$

All these non-zero entries are generated through dimension 3 terms in the Lagrangian for M_R . Now we add three complex scalar singlets $\chi_{\mu\tau}$, $\chi_{\mu\mu}$ and $\chi_{\tau\tau}$. The lepton number $U(1)_{L_\ell}$ assignments of these scalar singlets are given in Table 4. Under the action of Z_4 , $\chi_{\mu\mu} \leftrightarrow -\chi_{\tau\tau}$ and $\chi_{\mu\tau}$ remains invariant. These scalar fields generate Yukawa couplings $Y_6[(\nu_{\mu R}^T C^{-1}\nu_{\mu R})\chi_{\mu\mu} + (\nu_{\tau R}^T C^{-1}\nu_{\tau R})\chi_{\tau\tau}] + \text{H.c.}$ and $Y_7(\nu_{\mu R}^T C^{-1}\nu_{\tau R})\chi_{\mu\tau} + \text{H.c.}$. When the scalar singlet fields acquire non-zero VEVs one gets the desired form of M_R for class *IA*:

$$M_R = \begin{pmatrix} 0 & a & a \\ a & c+b & d \\ a & d & c-b \end{pmatrix}. \quad (41)$$

	$\chi_{\mu\tau}$	$\chi_{\mu\mu}$	$\chi_{\tau\tau}$
L_e	0	0	0
L_μ	-1	-2	0
L_τ	-1	0	-2

Table 4: Lepton number assignments of the scalar singlets.

5 Summary

We presented a detailed phenomenological analysis of neutrino mass matrices having one equality between cofactors and one vanishing cofactor. Such texture structures arise via

type-I seesaw mechanism when the Dirac neutrino mass matrix is diagonal with one equality between the elements and the right-handed Majorana neutrino mass matrix has hybrid textures. Out of the total sixty possible hybrid textures in the right-handed Majorana neutrino mass matrix only six are disallowed by the present neutrino oscillation data. Many of the allowed textures have constrained ranges for the unknown parameter M_{ee} , which will be probed in many forthcoming experiments for neutrinoless double beta decay. Some of the allowed textures have predictions for the Dirac-type CP-violating phase “ δ ”. Many textures also predict interesting correlations between M_{ee} and δ . In addition, there are predictions for the quadrant of the atmospheric mixing angle and we have compiled this information in Table 3. To show how such texture structures can be derived, we presented a flavor model for class *IA* using discrete flavor symmetries. At present, most of the hybrid textures of the inverse neutrino mass matrix can accommodate the available experimental data. Since most of the textures studied in this analysis have predictions for one or more presently unknown neutrino parameters, experimental results on these neutrino parameters such as the quadrant of θ_{23} , the value of Dirac-type CP-violating phase and the magnitude of the effective Majorana mass M_{ee} will help in deciding the viability of these type of textures in explaining neutrino masses and mixings.

Note: After the completion of this work a similar analysis with somewhat different results came to our notice [37].

Acknowledgements

R. R. G. acknowledges the financial support provided by the Council for Scientific and Industrial Research (CSIR), Government of India.

References

- [1] M. H. Ahn *et al.*, [K2K Collaboration], *Phys. Rev. Lett.* **90**, 041801 (2003), hep-ex/0212007; Y. Fukuda *et al.*, [Super-Kamiokande Collaboration], *Phys. Rev. Lett.* **81**, 1562 (1998), hep-ex/9807003; K. Eguchi *et al.*, [KamLAND Collaboration], *Phys. Rev. Lett.* **90**, 021802 (2003), hep-ex/0212021; T. Araki *et al.*, [KamLAND Collaboration], *Phys. Rev. Lett.* **94**, 081801 (2005), hep-ex/0406035; S. Abe *et al.*, [KamLAND Collaboration], *Phys. Rev. Lett.* **100**, 221803 (2008), arXiv:0801.4589 [hep-ex]; C. Arpesella *et al.*, [Borexino Collaboration], *Phys. Lett. B* **658**, 101 (2008), arXiv:0708.2251 [astro-ph]; B. T. Cleveland *et al.*, *Astrophys. J* **496**, 505 (1998); J. N. Abdurashitov *et al.*, [SAGE Collaboration], *J. Exp. Theor. Phys.* **95**, 181 (2002), astro-ph/0204245; W. Hampel *et al.*, [GALLEX Collaboration], *Phys. Lett. B* **447**, 127 (1999).
- [2] K. Abe *et al.* [T2K collaboration], *Phys. Rev. Lett.* **107**, 041801 (2011), arXiv:1106.2822 [hep-ex].

- [3] P. Adamson *et al.* [MINOS collaboration], *Phys. Rev. Lett.* **107**, 181802 (2011), arXiv:1108.0015 [hep-ex].
- [4] Y. Abe *et al.*, [Double Chooz collaboration], *Phys. Rev. Lett.* **108**, 131801 (2012), arXiv:1112.6353 [hep-ex].
- [5] F. P. An *et al.*, [Daya Bay collaboration], *Phys. Rev. Lett.* **108**, 171803 (2012), arXiv:1203.1669 [hep-ex].
- [6] Soo-Bong Kim, for RENO collaboration, *Phys. Rev. Lett.* **108**, 191802 (2012), arXiv:1204.0626 [hep-ex].
- [7] P. F. Harrison, D. H. Perkins and W. G. Scott, *Phys. Lett. B* **530**, 167 (2002), hep-ph/0202074; P. F. Harrison and W. G. Scott, *Phys. Lett. B* **535**, 163 (2002), hep-ph/0203209; Zhi-zhong Xing, *Phys. Lett. B* **533**, 85 (2002), hep-ph/0204049.
- [8] C. I. Low, R. R. Volkas, *Phys. Rev. D* **68**, 033007 (2003), hep-ph/0305243; C. S. Lam *Phys. Rev. D* **74**, 113004 (2006), hep-ph/0611017.
- [9] Paul H. Frampton, Sheldon L. Glashow and Danny Marfatia, *Phys. Lett. B* **536**, 79 (2002), hep-ph/0201008; Zhi-zhong Xing, *Phys. Lett. B* **530**, 159 (2002), hep-ph/0201151; Bipin R. Desai, D. P. Roy and Alexander R. Vaucher, *Mod. Phys. Lett. A* **18**, 1355 (2003), hep-ph/0209035; S. Dev, Sanjeev Kumar, S. Verma and S. Gupta, *Nucl. Phys. B* **784**, 103-117 (2007), hep-ph/0611313; S. Dev, S. Kumar, S. Verma and S. Gupta, *Phys. Rev. D* **76**, 013002 (2007), hep-ph/0612102; M. Randhawa, G. Ahuja, M. Gupta, *Phys. Lett. B* **643**, 175-181 (2006), hep-ph/0607074; G. Ahuja, S. Kumar, M. Randhawa, M. Gupta, S. Dev, *Phys. Rev. D* **76**, 013006 (2007), hep-ph/0703005; S. Kumar, *Phys. Rev. D* **84**, 077301 (2011), arXiv:1108.2137 [hep-ph]; P. O. Ludl, S. Morisi, E. Peinado, *Nucl. Phys. B* **857**, 411 (2012), arXiv:1109.3393 [hep-ph]; D. Meloni, G. Blankenburg, *Nucl. Phys. B* **867**, 749 (2013), arXiv:1204.2706 [hep-ph]; W. Grimus, P. O. Ludl, arXiv:1208.4515 [hep-ph].
- [10] H. Fritzsch, Zhi-zhong Xing, S. Zhou, *JHEP* **1109**, 083 (2011), arXiv:1108.4534 [hep-ph].
- [11] L. Lavoura, *Phys. Lett. B* **609**, 317 (2005), hep-ph/0411232; E. I. Lashin and N. Chamoun, *Phys. Rev. D* **78**, 073002 (2008), arXiv:0708.2423 [hep-ph]; E. I. Lashin, N. Chamoun, *Phys. Rev. D* **80**, 093004 (2009), arXiv:0909.2669 [hep-ph]; S. Dev, S. Verma, S. Gupta and R. R. Gautam, *Phys. Rev. D* **81**, 053010 (2010), arXiv:1003.1006 [hep-ph]; S. Dev, S. Gupta and R. R. Gautam, *Mod. Phys. Lett. A* **26**, 501-514 (2011), arXiv:1011.5587 [hep-ph]; T. Araki, J. Heeck and J. Kubo, *JHEP* **1207**, 083 (2012), arXiv:1203.4951 [hep-ph].
- [12] S. Dev, S. Gupta, R. R. Gautam and L. Singh, *Phys. Lett. B* **706**, 168 (2011), arXiv:1111.1300 [hep-ph].
- [13] S. Kaneko, H. Sawanaka and M. Tanimoto, *JHEP* **0508**, 073 (2005), hep-ph/0504074.

- [14] S. Dev, S. Verma and S. Gupta, *Phys. Lett.* **B 687**, 53-56 (2010), arXiv:0909.3182 [hep-ph].
- [15] Ji-Yuan Liu, Shun Zhou, arXiv:1304.2334 [hep-ph]
- [16] S. Dev, S. Gupta and R. R. Gautam, *Phys. Rev.* **D 82**, 073015 (2010) arXiv:1009.5501 [hep-ph].
- [17] P. Minkowski, *Phys. Lett.* **B 67**, 421 (1977); T. Yanagida, *Proceedings of the Workshop on the Unified Theory and the Baryon Number in the Universe* (O. Sawada and A. Sugamoto, eds.), KEK, Tsukuba, Japan, 1979, p. 95; M. Gell-Mann, P. Ramond, and R. Slansky, *Complex spinors and unified theories in supergravity* (P. Van Nieuwenhuizen and D. Z. Freedman, eds.), North Holland, Amsterdam, 1979, p.315; R. N. Mohapatra and G. Senjanovic, *Phys. Rev. Lett.* **44**, 912 (1980).
- [18] S. Dev, R. R. Gautam and Lal Singh *Phys. Rev.* **D 87**, 073011 (2013) arXiv:1303.3092 [hep-ph].
- [19] G. L. Fogli *et al.*, *Prog. Part. Nucl. Phys.* **57**, 742 (2006), hep-ph/0506083.
- [20] B. Pontecorvo, *Zh. Eksp. Teor. Fiz.* **33**, 549 (1957) [*Sov. Phys. JETP* **6** 429 (1957)].
- [21] C. Jarlskog, *Phys. Rev. Lett.* **55**, 1039 (1985).
- [22] M. Tortola, J. W. F. Valle and D. Vanegas, *Phys. Rev.* **D 86**, 073012 (2012), arXiv:1205.4018 [hep-ph].
- [23] C. Arnaboldi *et al.*, [CUORICINO collaboration], *Phys. Lett.* **B 584**, 260 (2004).
- [24] C. Arnaboldi *et al.*, *Nucl. Instrum. Methods Phys. Res., Sect. A* **518**, 775 (2004).
- [25] I. Abt *et al.*, [GERDA collaboration] hep-ex/ 0404039.
- [26] R. Gaitskell *et al.* [Majorana Collaboration] nucl-ex/0311013.
- [27] A. S. Barabash [NEMO Collaboration], *Czech. J. Phys.*, **52**, 567 (2002), nucl-ex/0203001.
- [28] M. Danilov *et al.*, *Phys. Lett.* **B 480**, 12 (2000), hep-ex/0002003.
- [29] H. V. Klapdor-Kleingrothaus, *et al.*, *Eur. Phys. J.* **A 12**, 147 (2001), hep-ph/0103062.
- [30] W. Rodejohann, *Int. J. Mod. Phys.* **E, 20**, 1833 (2011), arXiv:1106.1334 [hep-ph]
- [31] P. A. R. Ade *et al.* [Planck Collaboration], arXiv:1303.5076 [astro-ph]
- [32] W. Grimus, A. S. Joshipura, L.Lavoura and M. Tanimoto, *Eur. Phys. J.* **C 36**, 227 (2004), hep-ph/0405016.
- [33] Walter Grimus, Luis Lavoura, *J. Phys.* **G 31**, 693-702 (2005) hep-ph/0412283.

- [34] S. Dev, Shivani Gupta and R. R. Gautam, *Phys. Lett. B* **701**, 605-608 (2011), arXiv:1106.3451 [hep-ph].
- [35] M. Frigerio, S. Kaneko, E. Ma and M. Tanimoto *Phys.Rev. D* **71**, 011901 (2005), hep-ph/0409187.
- [36] W. Grimus, S. Kaneko, L. Lavoura, H. Sawanaka and M. Tanimoto, *JHEP* **01**, 110 (2006), hep-ph/0510326.
- [37] Weijian Wang, arXiv:1306.3556 [hep-ph].